Lanthanide Complexes with D-Penicillamine Methyl Ester: Formation Constants, Spectral and Thermal Properties

Shehab A. Sallam[a] and Marwa A. Mahmoud[b]

[a] Chemistry Department, Faculty of Science, Suez Canal University, Ismailia, Egypt
[b] Chemistry Department, Faculty of Petroleum and Mining Engineering, Suez Canal University, Suez, Egypt

Reprint requests to Dr. Shehab Sallam. E-mail:shehabsallam@yahoo.com

Z. Naturforsch. **61b,** 139 – 146 (2006); received October 10, 2005

The complex-formation of the lanthanide(III) cations with D-penicillamine methyl ester have been investigated in acidic and neutral media. The macroscopic protonation constants of the ligand and the formation constants of $[Ln{\cdot}Pme]^{2+}$, $[Ln{\cdot}(Pme)_2]^{+}$, $[Ln{\cdot}Pme{\cdot}OH]^{+}$ and $[Ln{\cdot}Pme{\cdot}(OH)_2]$ complexes have been determined from pH-metric data using BEST computer program. Species distribution diagrams of the complexes were obtained and plotted using SPE and SPEPLOT computer programs. Elemental analyses of the solid complexes indicate the formation of 1:1 metal:ligand species. Infrared spectra show that coordination takes place through the NH_2, the SH and the C=O groups of the ligand. The complexes decompose in four steps as shown by their TG and DTA analysis with the formation of $Ln_2(SO_4)_3$ as a final product. Activation energy values (ΔE_a) are correlated with the atomic radii of the metal ions. The mechanism of the thermal decomposition is proposed.

Key words: D-Penicillamine Methyl Ester, Lanthanide Complexes, Formation Constants, Infrared Spectra, Thermal Analysis

Introduction

Ligands containing both amine and thiol groups play an important role in technetium(V) chemistry as relevant to nuclear medicine [1]. Particularly, tetradentate N_2S_2 ligands such as diamine dithiols are the most valuable in the design of brain imaging ^{99m}Tc radiopharmaceuticals which should be neutral and lipophilic in order to be able to cross the blood brain barrier [2, 3].

The exclusive formation of such neutral N_2S_2 complexes by concerted action of a neutral and deprotonated amine-N donor atom is obviously interfered with or abolished by pendant carboxyl groups [4]. Compared with tetradentate N_2S_2 ligands having pendant carboxyl groups [4, 5], very few studies have been devoted to the composition and structure of oxo-complexes of Tc^{v} and Re^{v} with mercaptoamino-acids and their derivatives despite a continuous interest in the biological behavior of ^{99m}Tc complexes of cysteine and derivatives. Recently, profound solution studies of the oxorhenium(V) penicillamine complex have been described [6, 7] including the observation that the NH deprotonation does not occur in this system up to a very high pH value. Having studied the complexation behavior of Tc^{v} and Re^{v} with cystamine as the simple N,S donor building block of the ligand of interest, Kirch and his coworkers [8] have extended their investigations to D-penicillamine methyl ester. They have studied the reaction of oxorhenium(V) gluconate with D-penicillamine methyl ester (Pme) which yielded three neutral 1:2 complexes.

The hydrochlorides of cystamine ethyl ester and penicillamine methyl ester react with $Pd(PPh_3)_4$ to yield low symmetry complexes of palladium(II) that incorporate the N,S-aminothiolato ligand and triphenylphoshpine [9]. The reactivity of $PtCl_2$(2,2'-bipyridine) with penicillamine and penicillamine methyl ester in aqueous solution at pH 7 gives rise to $Pt_2(\mu\text{-}H_2Pen\text{-}S)_2(bpy)_2$ and $Pt_2(\mu\text{-}Pme\text{-}S)_2(bpy)_2$, complexes [10]. ^{1}H NMR spectroscopic studies of these complexes have indicated the complexes to have μ-S dimeric rather than η^2-N,S or η^2-O,S monomeric structures.

The rare-earth elements do not belong to the biometals. However, because of their similarity to Ca^{2+} and Mg^{2+}, Ln^{3+} ions can replace (or supplement) these biometals in some biological processes. The prospects of using complexes of rare-earth elements as drugs are based on this fact. Data on the composition and stability of the complexes of D-penicillamine methyl es-

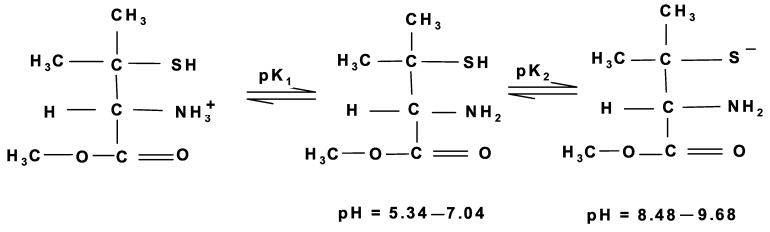

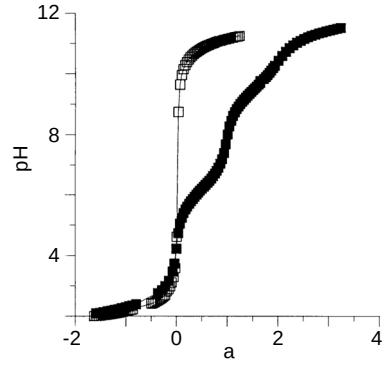

Fig. 1. Titration curve of the free D-penicillamine methyl ester in water medium, $[HNO_3] = 0.01$M, $[KOH] = 0.108$M, $I = 0.1$M $NaNO_3$, $V = 50$ ml and $t = 25$ °C. □ 0.01M HNO_3, ■ 0.004M Pme.

ter (Pme) with rare-earth elements in aqueous solution as well as in the solid state are unavailable. We describe here the results of potentiometric studies on the chelation of the biologically important Pme with the lanthanide series in water at ionic strength of 0.1M $NaNO_3$ and 25 °C. In addition, we have synthesized and characterized the first lanthanide complexes with Pme in which the metal atom is coordinated *via* the S atom, the NH_2 and the C=O groups simultaneously.

Results and Discussion

Solution chemistry of the D-penicillamine methyl ester

Potentiometric titrations of 0.006M solutions of Pme were performed in the pH range 4 – 11. Protonation reactions are possible for D-penicillamine methyl ester in the pH ranges indicated in the Scheme.

The mathematical model for the pH function was constructed on the basis of the equation of law of mass action and the material balance with respect to the basic components H^+ and Pme^-. The estimates of the constants $\beta_i (i = 1, 2, 3\ldots)$ were calculated with the aid of the BEST computer program [33] according to the non-linear least squares method.

The titration curve of Pme shows two clear inflections (Fig. 1). The first one is in the pH range 5.34 – 7.04 followed by the second which extend between pH 8.48 and 9.68. Because the acid strength of the ammonium group is comparable to that of the sulfohydryl group for a series of sulfohydryl and ammonium containing amino-acids, microscopic acid dissociation constants are required to characterize the acid-base chemistry at the molecular level [11]. Deprotonation may occur by two independent pathways: sulfohydryl followed by ammonium, or *vice versa*. Physically, there are two microscopic tautomers for the singly protonated macroscopic form, the site charged but electrically neutral tautomer (I) and the uncharged tautomer (II):

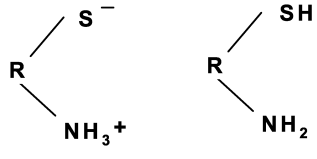

(I) (II)

Due to the charge differences between the two tautomers, it seems logical that the preferred deprotonation pathways will be highly dependent on specific solute-solvent and solvent-solvent interactions. The comparison with D-penicillamine [12] indicates that pK_1 (6.05) of Pme can be attributed to the ionization of the $-NH_3^+$ group ($pK_2 = 9.37$). The distribution of the equilibrium concentrations of D-penicillamine methyl ester molecular forms for an adequate mathematical model is shown in Fig. 2.

Solution chemistry of the Ln-Pme systems

The pH-metric titrations were carried out in a restricted range of pH values from 4.34 to 7.61, since the solutions became cloudy at higher pH values, probably due to the formation of sparingly soluble polymeric

Ion	pH-range	$\log\beta_{[Ln\cdot Pme]^{2+}}$	$\log\beta_{[Ln\cdot(Pme)_2]^{+}}$	$\log\beta_{[Ln\cdot PmeOH]^{+}}$	$\log\beta_{[Ln\cdot Pme\cdot(OH)_2]}$	n	σ
La^{3+}	4.63 – 7.16	4.02(0.1)	7.91(0.09)	−11.32(0.08)	−7.23(0.03)	58	0.013
Ce^{3+}	4.56 – 6.79	4.21(0.1)	8.35(0.11)	−11.53(0.06)	−7.41(0.07)	56	0.01
Pr^{3+}	4.36 – 6.60	4.29(0.1)	8.49(0.2)	−11.68(0.07)	−7.73(0.09)	62	0.01
Nd^{3+}	4.34 – 7.02	4.33(0.11)	8.54(0.13)	−11.86(0.05)	−7.69(0.08)	61	0.012
Sm^{3+}	4.37 – 7.61	4.27(0.1)	8.40(0.16)	−12.19(0.13)	−7.77(0.17)	62	0.023
Eu^{3+}	4.34 – 7.34	4.54(0.02)	8.45(0.04)	−12.48(0.11)	−7.59(0.13)	54	0.008
Gd^{3+}	4.37 – 6.95	4.34(0.05)	8.55(0.11)	−12.23(0.04)	−7.11(0.06)	60	0.014
Tb^{3+}	4.36 – 7.34	4.41(0.07)	8.71(0.11)	−12.33(0.09)	−7.34(0.8)	62	0.012
Dy^{3+}	4.62 – 7.27	4.59(0.03)	9.06(0.06)	−12.45(0.12)	−7.53(0.18)	60	0.009
Ho^{3+}	4.42 – 7.43	4.54(0.05)	8.92(0.09)	−12.35(0.56)	−7.6(0.63)	66	0.018
Er^{3+}	4.37 – 7.19	4.66(0.05)	9.14(0.11)	−12.33(0.32)	−7.23(0.03)	49	0.015
Tm^{3+}	4.47 – 7.24	4.49(0.14)	8.91(0.24)	−12.6(0.06)	−7.45(0.08)	58	0.016
Yb^{3+}	4.36 – 7.22	4.62(0.2)	8.99(0.36)	−12.59(0.08)	−7.44(0.1)	70	0.02
Lu^{3+}	4.37 – 7.18	4.96(0.01)	9.22(0.03)	−12.85(0.6)	−7.34(0.7)	98	0.004

Table 1. Formation constants* of lanthanide-D-penicillamine methyl ester complexes in water medium. [HPme] = 0.002M, $[Ln^{3+}]$ = 0.001M, [KOH] = 0.05M, I = 0.1M $NaNO_3$, V = 50 ml, t = 25 °C.

* Values in parentheses are error estimates.

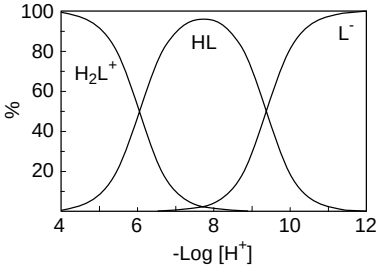

Fig. 2. Species distribution diagram of the D-penicillamine methyl ester.

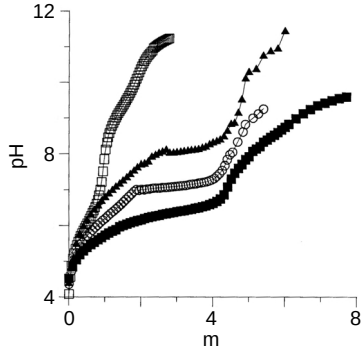

Fig. 3. Titration curves of the free Pme and its Ho^{3+} complex in water medium, [Pme] = 0.002M, $[Ln^{3+}]$ = 0.01M, [KOH] = 0.05M, I = 0.1M $NaNO_3$, V = 50 ml and t = 25 °C. □ 0.004M Pme, ▲ 0.001M Dy^{3+} + 0.002M Pme, ◯ 0.001M Tb^{3+} + 0.002M Pme, ■ 0.001M Yb^{3+} + 0.002M Pme.

complexes or hydroxo-species. The precipitates persist up to pH = 11. This phenomenon was also observed with lanthanide complexes of D-penicillamine (Pen) and D-penicillamine disulfide (Pds) [13, 14]. We have used dilute solutions of the lanthanide ions (0.001M) to avoid precipitation and formation of polynuclear or hydroxo-complexes. Also, the calculations were restricted to data obtained before precipitation. Titration in small pH regions was also carried out in complexation of Ln(III) with each of aspartic and malic acids [15].

The mathematical model for the pH function was constructed on the basis of the law of mass action of the molecular species and the material balance with respect to the components Ln^{3+}, H^+ and Pme^-. The protonation constants of the Pme as well as the formation constants of the molecular species taken from [34] were introduced into the model as determined quantities. The estimates of the formation constants are presented in Table 1. The two forms of D-penicillamine methyl ester, HPme and Pme^-, can form complexes with the metal cations. Complexes $[Ln\cdot HPme]^{3+}$ will certainly be unstable, since protonation blocks the amino group of the Pme ligand. The complex $[Ln\cdot Pme]^{2+}$, in which the Ln^{3+} ion can appear in the ring 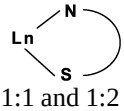

will be the most stable. Complexes with 1:1 and 1:2 molar ratios of Ln^{3+}:Pme were titrated against 0.05 M KOH. The data are plotted in Fig. 3.

The titration curves show a break at m = 2 for all 1:1 systems, which can be explained by the release of two protons from the protonated form of the ligand molecules and formation of 1:1 metal:ligand complexes. The 1:2 Ln:Pme systems show titration curves which indicate the release of four titratable protons per metal ion, and further there is a break in each of the curves at m = 2 and m = 4 indicating the formation of both 1:1 and 1:2 complexes. The complex forming equilibria are represented as follows:

$$Ln^{3+} + H_2Pme^+ \rightarrow [Ln\cdot Pme]^{2+} + 2H^+,$$

$$\beta_{[Ln\cdot Pme]^{2+}} = \frac{[Ln\cdot Pme]^{2+}\cdot[H^+]^2}{[Ln^{3+}]\cdot[H_2Pme^+]}$$

	$\log\beta_1$			$\log\beta_2$		
	Pen [13]	Pme	Pds [14]	Pen [13]	Pme	Pds [14]
La^{3+}	5.72(0.04)	4.02(0.1)	4.45(0.04)	10.84(0.12)	7.91(0.09)	8.60(0.10)
Ce^{3+}	5.50(0.03)	4.21(0.1)	4.40(0.02)	10.83(0.02)	8.35(0.11)	8.63(0.11)
Pr^{3+}	5.47(0.02)	4.29(0.1)	4.43(0.02)	10.63(0.09)	8.49(0.2)	8.65(0.02)
Nd^{3+}	5.85(0.02)	4.33(0.11)	4.45(0.02)	10.92(0.03)	8.54(0.13)	8.67(0.02)
Sm^{3+}	6.07(0.02)	4.27(0.1)	4.49(0.01)	11.42(0.12)	8.40(0.16)	8.75(0.07)
Eu^{3+}	6.06(0.02)	4.54(0.02)	4.52(0.01)	11.44(0.1)	8.45(0.04)	8.61(0.07)
Gd^{3+}	6.05(0.03)	4.34(0.05)	4.31(0.02)	11.26(0.16)	8.55(0.11)	8.44(0.11)
Tb^{3+}	6.06(0.02)	4.41(0.07)	4.60(0.02)	11.62(0.1)	8.71(0.11)	8.89(0.02)
Dy^{3+}	6.07(0.05)	4.59(0.03)	4.62(0.01)	11.62(0.16)	9.06(0.06)	8.92(0.06)
Ho^{3+}	6.06(0.04)	4.54(0.05)	4.66(0.02)	11.80(0.2)	8.92(0.09)	8.97(0.09)
Er^{3+}	5.94(0.03)	4.66(0.05)	4.68(0.01)	11.60(0.08)	9.14(0.11)	9.0(0.03)
Tm^{3+}	5.91(0.07)	4.49(0.14)	4.72(0.02)	11.78(0.2)	8.91(0.24)	9.05(0.09)
Yb^{3+}	5.92(0.08)	4.62(0.2)	4.71(0.01)	11.62(0.08)	8.99(0.36)	9.03(0.05)
Lu^{3+}	5.93(0.03)	4.96(0.01)	4.72(0.03)	11.46(0.2)	9.22(0.03)	9.04(0.12)

Table 2. Comparison of the formation constants* of the lanthanide complexes of Pen, Pme and Pds.

* Values in parentheses are error estimates.

$$Ln^{3+} + 2\,H_2Pme^+ \rightarrow [Ln\cdot(Pme)_2]^+ + 4H^+,$$

$$\beta_{[Ln\cdot(Pme)_2]^+} = \frac{[Ln\cdot(Pme)_2]^+\cdot[H^+]^4}{[Ln^{3+}]\cdot[H_2Pme^+]^2}$$

The formation constants $\log\beta_{[Ln\cdot Pme]^{2+}}$ and $\log\beta_{[Ln\cdot(Pme)_2]^+}$ were found to increase in the order $Pr^{3+} < Nd^{3+} < Eu^{3+} < Dy^{3+} < Er^{3+} < Lu^{3+}$ which is in accordance with the order of increasing acidity of the metal ions. $[Ln\cdot(Pme)_3]$ type complexes were not observed in the pH range in which the titration was performed because of their low stability. With donor oxygen atoms present in Pen and Pds, the "harder" lanthanide(III) ion Lewis acids should preferentially bond to these sites. Table 2 compares the values of $\log\beta$ obtained for the chelates of Pme with their analogues of Pen and Pds. We conclude the following:

1) Ln(III) chelates of Pen have the higher formation constants, may be due to the bonding to all three donor atoms O, N and S.

2) In Pds chelates, the values of the formation constants are lower than for Pen chelates. This may be due to the fact that in Pds, only O and N are available for bonding since S is involved in the disulfide bonding.

3) In Pme chelates, the metals are only bonded to the N and S atoms, since the carboxylic group is esterified. It is thus expected that chelates of Pme with Ln^{3+} must have formation constants that are lower than those of the analogues with Pen and comparable to Pds chelates as confirmed by data in Table 2.

It is probable that in the Ln^{3+}:Pme complexes, the oxygen atom of the ester group entertains weak bonding towards Ln^{3+} which raises the formation constant values. In general, amino acids show weak binding to lanthanide cations. Formation constant values are always low and variations for different amino acids are quite small. The interactions are mostly determined by electrostatic interaction [16].

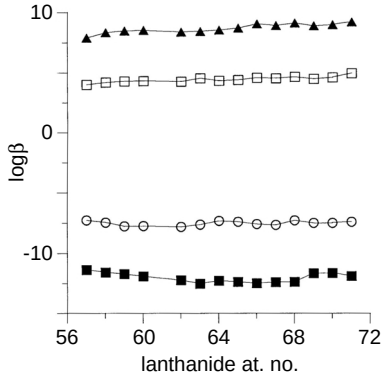

Fig. 4. Variation of $\log\beta$ of the Ln-Pme complexes with the lanthanide atomic number.
□ $\log\beta_{[Ln\cdot Pme]^{2+}}$, ▲ $\log\beta_{[Ln\cdot(Pme)_2]^+}$, ◯ $\log\beta_{[Ln\cdot Pme\cdot OH]^+}$, ■ $\log\beta_{[Ln\cdot Pme\cdot(OH)_2]}$.

Fig. 4 depicts the variation of $\log\beta$ values of the Ln^{3+}:Pme complexes as a function of the Ln atomic number. The pattern of these plots shows a slight increase of $\log\beta$ versus atomic number which is indicative of the predominantly ionic nature of bonding between Ln^{3+} and the Pme ligand [17]. Several complexing systems have been shown to have such a mode of variation [18, 19].

The different magnitudes of the formation constants of the complexes are manifested in different concentrations of the complex species. The concentration distribution of the Ln(III)-Pme complexes in solution as a function of pH has been determined and plotted by means of SPE and SPEPLOT

computer programs [33]. The most stable complexes are $[Ln{\cdot}Pme]^{2+}$, $[Ln{\cdot}(Pme)_2]^{+}$, $[Ln{\cdot}Pme{\cdot}OH]^{+}$ and $[Ln{\cdot}Pme{\cdot}(OH)_2]$. The concentrations of the complex species reflect their different formation constants. A maximum proportion of $[Ln{\cdot}Pme]^{2+}$ species is obtained with Lu^{3+} (40.8%) at pH 7.5 followed by Ho^{3+} (35.1%) at pH 7.8 and Eu^{3+} (32.1%) at pH 7.7. The same trend is obtained for $[Ln{\cdot}(Pme)_2]^{+}$ which has a species maximum with Lu^{3+} (45.8%) at pH 7.5, Ho^{3+} (34.5%) at pH 8.3% and Eu^{3+} (27.1%) at pH 8.1. Minimum proportions are obtained for $[Pr{\cdot}Pme]^{2+}$ and $[Pr{\cdot}(Pme)_2]^{+}$ (5.5% and 1.4%) at pH 6.9 and 7, and for $[Gd{\cdot}Pme]^{2+}$ and $[Gd{\cdot}(Pme)_2]^{+}$ (11.3% and 1.5%) at pH 7.1 and 7.4. For the hydroxo-complex $[Ln{\cdot}Pme{\cdot}OH]^{+}$, the maximum concentration was obtained with Tm^{3+} and Yb^{3+} (27.5 and 27.8%) at pH 7.6. It is concluded that the heavier lanthanides form more stable complexes than the lighter ones.

Solid Ln-Pme complexes

The complexes of Sm^{3+}, Gd^{3+} and Yb^{3+} with the Pme ligand are white solids, insoluble in alcohol, acetone, diethyl ether, pyridine, and also DMF and DMSO. Elemental analyses of the complexes show a 1:1 metal:ligand stoichiometry. It is shown that Pme is functioning as an uninegatively charged chelating agent.

Infrared spectra of the Ln-Pme complexes

The results of the IR measurements of D-penicillamine methyl ester (Pme) and its Pr, Gd and Yb complexes – where the band assignments of the guide bands (those affected by coordination) – have been given. In the higher frequency region, for Pme a strong broad band at 2925 cm^{-1} with a shoulder at 3177 cm^{-1}, is assigned to $\nu(NH_2)$ vibration [20–22]. ν(SH) appears as a strong sharp band in the spectrum of the Pme at 2489 cm^{-1}. A weak absorption is noticed at 1950 cm^{-1} which is characteristic of many amino-acid hydrochlorides [23]. The carbonyl group stretching vibration has a strong sharp absorption at 1743 cm^{-1}. $\delta(NH_2)$ is obtained as sharp medium band at 1579 cm^{-1}.

The potentially active sites which may participate in coordination are: the NH_2, the C=O and the SH groups. This mode of chelation is supported by the following evidences:

a) The stretching vibration band $\nu(NH_2)$ is shifted to higher wavenumber (to the region 3306–3225 cm^{-1}) in the spectra of the complexes. The in-plane deformation band $\delta(NH_2)$ is shifted to the 1590–1603 cm^{-1} region, compared to the free Pme spectra [24–26].

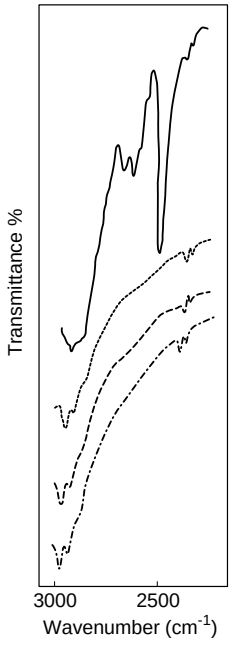

Fig. 5. Infrared spectra of the free Pme and its complexes.
— free Pme,
... $[Pr{\cdot}Pme{\cdot}(NO_3)_2] \cdot 2\,H_2O$,
- - - $[Gd{\cdot}Pme{\cdot}(NO_3)_2]{\cdot}3\,H_2O$ and
-·- $[Yb{\cdot}Pme{\cdot}(NO_3)_2]{\cdot}2\,H_2O$.

b) The sharp medium band assigned to ν(SH) has completely disappeared in the spectra of the complexes as shown in Fig. 5, indicating the ionization of the SH group.

c) The ν(C=O) frequency in the spectrum of Pme is shifted to lower wavenumbers (1629–1637 cm^{-1}).

Literature data for the synthesis and characterization of Pme complexes are scarce. Kirch *et al.* [8] have shown that the reaction of oxorhenium(v) gluconate with D-penicillamine methyl ester yields three neutral 1:2 complexes. One of these complexes is the mixed ligand species $[ReO\{SC(CH_3)_2CH(CO_2CH_3)NH_2\}\{SC(CH_3)_2CH(CO_2)NH_2\}]$ which was obtained in aqueous solutions. It contains bidentate D-penicillamine methyl ester and tridentate D-penicillamine. The other two complexes show a deprotonated and a neutral nitrogen donor group in the $ReO(NS)_2$ system in an unusual coordination mode for bidentate N,S ligands. Infrared spectra (in KBr) of the last two complexes show very strong absorption bands at 1732 and 1728 cm^{-1} assigned to the free, noncoordinated carbonyl ester group. Infrared data of our complexes show the shift to the 1629–1637 cm^{-1} range, suggesting the coordination of the carbonyl ester group.

Table 3. DTA, TGA and DTG data of the lanthanide-D-penicillanmine methyl ester complexes.

Complexes	DTA results					TGA and DTG results					
	Temp. range	t °C	ΔH J/mol	E_a	Process	Temp. range	DTG °C	Wt. loss found	Wt. loss calcd.	Type of loss	Residue
$[Pr{\cdot}Pme{\cdot}(NO_3)_2]$	33 – 95	65 endo.	96	79	Dehydration	34 – 166	67	7.42	7.2	$2H_2O$	
$\cdot 2\ H_2O$	217 – 320	277 exo.	−372	197	Coordination sphere	216 – 377	264	28.02	30.20	$2CH_3+2NO_3$	
	329 – 398	340 exo.	−318	484	Partial decomposition	423 – 493	457	6.05	6.4	CH_3OH	
	453 – 556	522 exo.	−229	486	Final decomposition	525 – 624	560	58.51	57.24	L	$Pr_2(SO_4)_3$
$[Gd{\cdot}Pme{\cdot}(NO_3)_2]$	33 – 88	69 endo.	101	67	Dehydration	31 – 100	63	9.91	10.10	$3H_2O$	
$\cdot 3\ H_2O$	220 – 344	283 exo.	−338	123	Coordination sphere	230 – 338	256	27.44	28.78	$2CH_3+2NO_3$	
	377 – 425	400 exo.	−319	211	Partial decomposition	340 – 459	400	5.8	5.98	CH_3OH	
	591 – 651	672 exo.	−197	440	Final decomposition	620 – 675	639	56.85	56.32	L	$Gd_2(SO_4)_3$
$[Yb{\cdot}Pme{\cdot}(NO_3)_2]$	33 – 100	63 endo.	142	50	Dehydration	43 – 104	67	6.76	7.03	$2H_2O$	
$\cdot 2\ H_2O$	245 – 329	289 exo.	−405	119	Coordination sphere	211 – 333	258	28.59	28.96	$2CH_3+2NO_3$	
	338 – 409	382 exo.	−335	122	Partial decomposition	353 – 474	412	6.19	6.01	CH_3OH	
	645 – 779	729 exo.	−168	423	Final decomposition	696 – 800	767	58.18	59.63	L	$Yb_2(SO_4)_3$

The presence of coordinated nitrate ions is indicated by three medium bands in the 1379 – 1386, 1181 – 1191 and 1018 – 1027 cm^{-1} regions, respectively, due to the ν_5, ν_1 and ν_2 vibrations of nitrate ions of C_{2v} symmetry [27]. Since $\nu_5 - \nu_1$ are in the 188 – 198 cm^{-1} range, the nitrate ion may coordinate in monodentate or bidentate fashion [27].

Thermal analysis of the Ln-Pme complexes

The TGA. and DTG curves of the $[Pr{\cdot}Pme{\cdot}(NO_3)_2]{\cdot}2\,H_2O$, $[Gd{\cdot}Pme{\cdot}(NO_3)_2]{\cdot}3\,H_2O$ and $[Yb{\cdot}Pme{\cdot}(NO_3)_2]{\cdot}2\,H_2O$ complexes are shown in Fig. 6. The complexes are decomposed in four stages. The initial mass losses observed correspond to the release of 2 and 3 moles of water. The next decomposition stages are due mainly to loss of nitrate ions. This is confirmed by the infrared spectra of the decomposition products, which showed the disappearance of the bands in the 1379 – 1386, 1188 – 1191 and 1026 – 1027 cm^{-1} ranges, respectively, characteristic for the nitrate ion. The final stages start at 525, 620 and 696 °C and come to an end at 624, 675 and 800 °C with DTG maxima at 560, 639 and 767 °C, respectively, which indicate the formation of $Pr_2(SO_4)_3$, $Gd_2(SO_4)_3$ and $Yb_2(SO_4)_3$, respectively, as confirmed by IR spectroscopy [27 – 29] (Fig. 7).

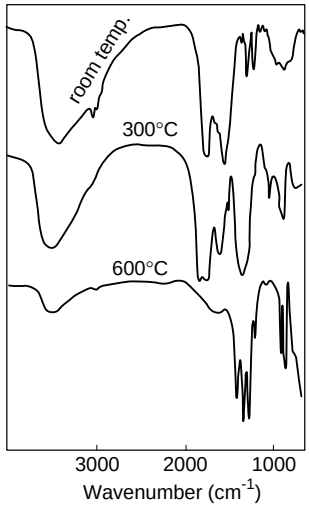

Fig. 7. Infrared spectra of heated samples of the $[Gd{\cdot}Pme{\cdot}(NO_3)_2]{\cdot}3\,H_2O$ complex.

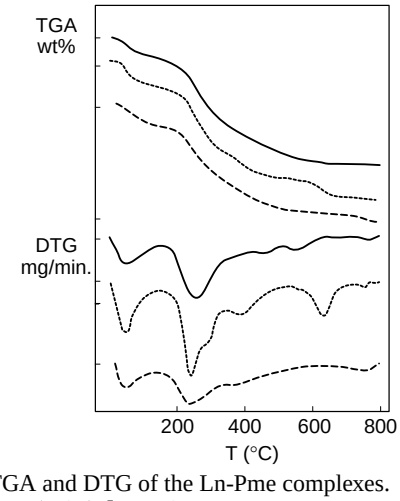

Fig. 6. TGA and DTG of the Ln-Pme complexes.
— $[Pr{\cdot}Pme{\cdot}(NO_3)_2]{\cdot}2\,H_2O$,
··· $[Gd{\cdot}Pme{\cdot}(NO_3)_2]{\cdot}3\,H_2O$ and
- - - $[Yb{\cdot}Pme{\cdot}(NO_3)_2]{\cdot}2\,H_2O$.

All transitions in the DTA curves are corresponding to the transitions observed in the TGA curves. The enthalpies of dehydration have the values of 96, 101 and 142 *J*/mol, respectively, which indicate stronger bonding of the water molecule in the $[Yb{\cdot}Pme{\cdot}(NO_3)_2]{\cdot}2\,H_2O$ complex. The enthalpies of the partial decomposition at the following stages have the values of 372, 338,

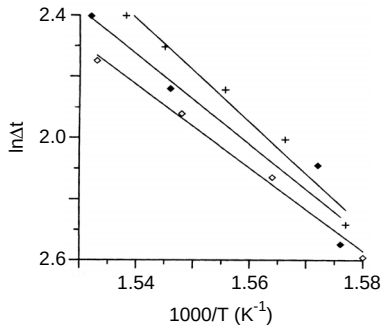

Fig. 8. Linearization curves of the Ln-Pme complexes (third decomposition step). + $[Pr{\cdot}Pme{\cdot}(NO_3)_2]{\cdot}2\,H_2O$, ♦ $[Gd{\cdot}Pme{\cdot}(NO_3)_2]{\cdot}3\,H_2O$, ◊ $[Yb{\cdot}Pme{\cdot}(NO_3)_2]{\cdot}2\,H_2O$.

405 and 318, 319, 335 J/mol, respectively, in the order $[Yb{\cdot}Pme{\cdot}(NO_3)_2]{\cdot}2\,H_2O > [Gd{\cdot}Pme{\cdot}(NO_3)_2]\cdot 3\,H_2O > [Pr{\cdot}Pme{\cdot}(NO_3)_2]{\cdot}2\,H_2O$ suggesting a correlation with the ionic radius Yb < Gd < Pr. Exothermic peaks at 522, 672 and 729 °C indicate final decomposition of the complexes with formation of metal sulfate as final product.

The activation energy E_a of the thermal decomposition reaction has been elucidated by the method of Piloyan [30]. The linear relationship of $\ln\Delta t$ versus 1000/T is given in Fig. 8. The activation energy of Pr(III), Gd(III) and Yb(III) complexes is expected to increase proportional to the decrease in the ionic radius [31]. This rule, however, appears to be not valid in the case of the Ln-Pme complexes: $[Yb{\cdot}Pme{\cdot}(NO_3)_2]{\cdot}2\,H_2O$ has a lower value of E_a than $[Pr{\cdot}Pme{\cdot}(NO_3)_2]{\cdot}2\,H_2O$ for the first, second and third decomposition steps. This may be attributed to steric reasons due to the presence of $-OCH_3$ substituent in the ligand molecule.

Experimental Section

D-Penicillamine methyl ester was obtained from Sigma. Other chemicals were A.R. grade reagents and were used without further purification.

Preparation of the solid complexes

All complexes were prepared according to the following procedure. Pme dissolved in a minimum amount of water was added slowly with stirring to the metal nitrate (B.D.H.) that was also dissolved in a minimum amount of water. The pH of the mixture was increased to 5.5 by addition of dilute KOH solution drop by drop with stirring and heating on a water bath. After one hour, the formed precipitate was filtered, washed with distilled water and dried under vacuum over $CaCl_2$. Elemental analyses and infrared data (KBr) for $[Pr{\cdot}Pme{\cdot}(NO_3)_2]{\cdot}2\,H_2O$ (499.527): calcd. C 14.42, N 8.4, H 3.2, Pr 28.2; found C 14.7, N 8.52, H 3.96, Pr 28.33. – IR: υ = 3428 (OH), 3225 $(NH_2)_{as}$, 1629 (C=O), 1590 (δNH_2), 1379, 1181, 1018 (NO_3^-). For $[Gd{\cdot}Pme{\cdot}(NO_3)_2]{\cdot}3\,H_2O$ (534.86): calcd. C 13.49, N 7.86, H 3.37, Gd 29.45; found C 13.65, N 7.93, H 3.69, Gd 29.57. – IR: υ = 3410 (OH), 3225 $(NH_2)_{as}$, 1637 (C=O), 1603 (δNH_2), 1386, 1188, 1026 (NO_3^-). For $[Yb{\cdot}Pme{\cdot}(NO_3)_2]{\cdot}2\,H_2O$ (531.66): calcd. C 14.73, N 7.89, H 3.0, Yb 32.54; found C 14.91, N 7.81, H 3.21, Yb 32.39. – IR: υ = 3429 (OH), 3306 $(NH_2)_{as}$, 1637 (C=O), 1595 (δNH_2), 1379, 1191, 1027 (NO_3^-).

Equipment

C, H and N contents were measured using a Perkin-Elmer 2400 elemental analyzer at the Microanalytical Center of Cairo University. Infrared spectra of the ligand and its complexes were obtained with a Bruker Vector22 spectrophotometer. TGA, DTG and DTA analysis were recorded using a Shimadzu-50 thermal analyzer in a flow of nitrogen (30 ml/min.) with a heating rate 10 °C/min. Metal content of the complexes was obtained by titration with EDTA against xylenol orange as indicator at pH 4 using acetate buffer.

Potentiometric titrations

Solutions of the metal nitrates were standardized by EDTA titration. KOH solution was standardized against potassium hydrogen phthalate solution and the carbonate content was checked using Gran's plot [32].

Potentiometric measurements were carried out using a Fischer Accumet 825MP pH-meter equipped with a Fischer combined glass electrode. The pH-meter was standardized with phthalate and phosphate buffers before titrations. Titrant solutions were added using a Fischer-455 automatic burette. Sample solutions were titrated in a double-walled glass cell maintained at constant temperature (25 °C) using a Fischer Scientific Isotemp Refrigerated Circulating Bath under continuos flow of nitrogen. Titrations were performed over the desired pH range using 50 ml samples in a medium of constant ionic strength (5 ml 1M $NaNO_3$). The following solutions were titrated:

(i) 5 ml 0.1M HNO_3 + 40 ml H_2O.
(ii) 5 ml 0.04M Pme + 5 ml 0.1M HNO_3 + 35 ml H_2O.
(iii) 5 ml 0.04M Pme + 40 ml H_2O.
(iv) 5 ml 0.02M Pme + 5 ml 0.01M Ln^{3+} + 5 ml 0.1M HNO_3 + 30 ml H_2O.
(v) 5 ml 0.02M Pme + 5 ml 0.01M Ln^{3+} + 35 ml H_2O.

Equilibrium pH values were determined at every incremental addition of standard KOH to the solutions. The pH values were plotted as a function of (m) values or (a) values (m is the ratio of moles of base added per mole of metal ion

present and a is the ratio of moles of base added per mole of ligand present). The value of $K_w([H^+]\cdot[OH^-])$ used in the computations was calculated from the strong base solution and was found to be 13.83 ± 0.02 at 25 ± 0.01 °C at an ionic strength of 0.1M $NaNO_3$.

Calculations

The protonation constants of the ligand and the formation constants of the complexes were computed from the titration data using PKAS and BEST computer programs [33]. Species distribution diagrams were calculated from the formation constants and plotted using SPE and SPEPLOT computer programs [33]. The model selected was that which gave the best statistical fit to the titration data and was consistent with chemical logic. The computation of the formation constants was based on the minimization of the sigma fit , however, error estimates were performed by propagation of error analysis. Hydrolysis of lanthanide salts was taken into account in the calculation of the formation constants [34].

[1] B. Johannsen, H. Spies, Top. Curr. Chem. **17**, 77 (1996).
[2] L. A. Epps, H. D. Burns, S. Z. Lever, H. W. Golfarb, H. N. Wagner (Jr.), Appl. Radiat. Isot. **38**, 661 (1987).
[3] D. S. Edwards, E. H. Cheesman, M. W. Watson, L. J. Maheu, S. A. Nguyen, E. Dimitre, T. Nason, A. D. Watson, R. Walovitch, in M. Nicolini, G. Bandoli, U. Mazzi (eds): Technetium and Rhenium in Chemistry and Nuclear Medicine, p. 433, Cortina International, Verona Raven Press, New York (1990).
[4] L. G. Marzilli, M. G. Banaszcyk, L. Hansen, Z. Kuklenyik, R. Cini, A. Taylor (Jr.), Inorg. Chem. **33**, 4850 (1994).
[5] L. Hansen, M. Lipowska, A. Taylor (Jr.), L. G. Marzilli, Inorg. Chem. **34**, 3579 (1995).
[6] L. Hansen, X. Xu, K. T. Yue, Z. Kuklenyik, A. Taylor (Jr.), G. L. Marzilli, Inorg. Chem. **35**, 1958 (1996).
[7] L. Hansen, X. Xu, K. T. Yue, A. Taylor (Jr.), L. G. Marzilli, Inorg. Chem. **35**, 2785 (1996).
[8] S. Kirch, B. Noll, H. Spies, P. Leibnitz, D. Scheller, T. Krueger, B. Johannsen, J. Chem. Soc. Dalton Trans. **3**, 455 (1998).
[9] J. Real, M. Pagès, A. Polo, J. Piniella, Á. Álvarez-Larena, Chem. Commun. 277 (1999).
[10] K. A. Mitchell, C. M. Jensen, Inorg. Chem. **34**, 4441 (1995).
[11] L. Pillai, P. D. Boss, M. S. Greenberg, J. Soln. Chem. **8**, 3177 (1969).
[12] N. A. Atanova, N. A. Dobryanina, Yu. A. Kir'yanov, L. S. Nikolaeva, V. S. Sultanova, Russ. J. Inorg. Chem. **41**, 233 (1996); S. Runar, W. L. Aaseth, J. Inorg. Biochem. **19**, 301 (1983); M. J. Willes, D. R. Williams, Inorg. Chim. Acta **80**, 135 (1983); E. J. Kuchiuskas, J. Rosen, Arch. Biochem. Biophys. **97**, 370 (1962); H. Kõszegi-Szalai, T. L. Paál, Talanta **48**, 293 (1999).
[13] Sh. A. Sallam, K. M. Bahgat, A. Z. El-Tanany, M. A. Mahmoud, J. Coord. Chem., accepted for publication (November 2005).
[14] M. A. Mahmoud, M. Sc. Thesis, Suez Canal University (2005).
[15] R. Prados, L. G. Stadtherr, H. Donato (Jr.), R. B. Martin, J. Inorg. Nucl. Chem. **36**, 689 (1974).
[16] A. E. Martell, R. D. Hancock, Metal Complexes in Aqueous Solutions, Plenum Press, New York (1996).
[17] C. Kremer, J. Torres, S. Dominguez, A. Medros, Coord. Chem. Rev. **249**, 567 (2005).
[18] G. R. Choppin, E. Chebaugh, J. Inorg. Nucl. Chem. **17**, 2301 (1978).
[19] I. Grenthe, W. C. Fernelius, J. Am. Chem. Soc. **82**, 6258 (1969).
[20] G. Zerbi, C. Alberti, Spectrochim. Acta **18**, 407 (1962); **19**, 1261 (1963).
[21] E. Borello, A. Zecchina, Spectrochim. Acta **19**, 1703 (1963).
[22] H. W. Thompson, D. L. Nicholson, L. N. Short, Discuss. Faraday Soc. **9**, 222 (1950).
[23] L. J. Bellamy, The Infrared Spectra of Complex Molecules, Chapman and Hall, London (1973).
[24] B. M. Gatehouse, S. E. Livingstone, R. S. Nyholm, J. Chem. Soc. 4222 (1957); J. Inorg. Nucl. Chem. **8**, 75 (1958).
[25] V. Aletras, N. Hadjiliadis, B. Lippert, Polyhedron **11**, 1359 (1992).
[26] A. S. Zidan, A. I. El-Said, M. S. El-Meligy, A. A. Aly, O. F. Mohamed, J. Therm. Anal. **26**, 665 (2000).
[27] K. Nakamoto, Infrared and Raman Spectra of Inorganic and Coordination Compounds, 3rd Ed. , John Wiley & Sons, New York (1992).
[28] V. P. Surgutskii, V. I. Gaivoronskii, V. V. Serebrennikov, Zh. Neorg. Khim. 13, 1010 (1968).
[29] R. D. Baybarz, J. A. Fahey, R. G. Haire, J. Inorg. Nucl. Chem. 36, 2023 (1974).
[30] G. O. Piloyan, I. D. Ryabchikov, O. S. Novikova, Nature **5067**, 1229 (1966).
[31] A. M. Donia, Thermochim. Acta **320**, 187 (1998).
[32] G. Gran, Analyst **77**, 661 (1952).
[33] A. E. Martell, R J. Mutekaities, Determination and Use of Stability Constants, VCH, New York (1992).
[34] G. D. Klungness, R. H. Byrne, Polyhedron **19**, 99 (2000).